



Critical Review of the Global Chemical Kinetics of Cellulose Thermal Decomposition

Alan K. Burnham,^{*,†,§} Xiaowei Zhou,[‡] and Linda J. Broadbelt[‡]

[†]American Shale Oil LLC, Rifle, Colorado 81650, United States

[‡]Department of Chemical and Biological Engineering, Northwestern University, Evanston, Illinois 60208, United States

ABSTRACT: Historical models for cellulose pyrolysis and mathematical approaches to kinetic analysis are reviewed with the objective of identifying the correct global chemical kinetic models and parameters for cellulose pyrolysis. In most recent experiments, cellulose pyrolysis clearly has sigmoidal reaction character, which is consistent with one of a sequential, nucleation–growth, or random-scission global model. The apparent activation energy of ~ 47 kcal/mol is consistent with mechanistic modeling if one allows catalytic acceleration of the concerted initiation reaction. There is a possibility that part of the sigmoidal character is due to adsorption effects at low pyrolysis temperatures, but further work is required to resolve this issue. Reasons are given for why fitting data at a single heating rate to a first-order reaction model gives incorrect results.

■ INTRODUCTION

After decades of research, progress is being made on both the fundamental mechanism of cellulose pyrolysis and simpler global kinetic models. Even so, there are historical disagreements concerning the existence of “active” cellulose, whether the decomposition is first order or not, and the role of heat and mass transfer on the observed kinetics that have not yet been fully resolved by this progress. The objective of this paper is to show consistency of the current state of the art for mechanistic modeling with an improved global model that might be considered an evolutionary improvement of previous models. The hope, of course, is that this paper will direct the field toward more productive experiments and development efforts on global and mechanistic models.

This paper reviews the development of global conceptual models in general terms, the relationship of these models to common mathematical models, the possible validity of these various approaches based on what has been learned recently by detailed mechanistic modeling, and pitfalls in experimental measurements that may confuse the calibration of global models. It presents a reanalysis and calibration of a few simple global models based on the best available data and understanding.

This paper is not intended to be a comprehensive review of all previous work on cellulose and biomass pyrolysis, as there are already many hundreds of papers on the subject with diverse results and conclusions. More comprehensive reviews of biomass pyrolysis are available,^{1–3} and perusal of those reviews reveal a huge discrepancy in the apparent activation energy (E_a) ranging from 10 to 63 kcal/mol and an associated variation in the pre-exponential factor (A) of 10 to 10^{21} s^{−1}. Instead, only selected papers that address specific issues will be discussed, but hopefully these papers capture all the important aspects of previous work and the central issues relating to the mechanism and the variation in apparent A and E_a . However, literature is included from other application areas (e.g., fossil fuels, synthetic polymers, inorganic crystals) that is directly relevant to

cellulose pyrolysis issues but is not commonly recognized in the cellulose literature.

■ HISTORICAL GLOBAL MODELS

The first well-founded global kinetic model for cellulose pyrolysis is generally considered to be the Broido–Shafizadeh model.⁴ Two important features of this model are (1) a reaction intermediate (“active” cellulose in this case) between the starting material and the final products and (2) two final product pathways with different activation energies that enable a temperature-dependent ratio of volatiles and char. The latter characteristic is not unique to cellulose—it is also observed in other synthetic polymers and geopolymers.

Subsequently, Diebold⁵ proposed an expanded mechanism. This mechanism has two independent pathways for dehydration and char formation and two secondary reaction pathways for the primary vapors, but the core of the reaction model is still the same, namely, that there is a distinct reaction intermediate between cellulose and the primarily volatile products.

Char formation is a function of heating rate and volatiles continue to be formed from the char as it is heated to higher temperatures than needed to completely decompose the cellulose structure.^{6–8} However, that aspect is secondary to the primary mass loss mechanism, which accounts for 90% or more of the volatile products. Furthermore, reactions for char formation can be added onto the core of the reaction model. Consequently, the central question for constructing a global model is whether there truly is a reaction intermediate (not restricted in meaning to “active” cellulose) between cellulose and the primary volatiles, of which levoglucosan is the primary species.^{9,10}

There are three possible answers: no, yes, and sometimes.

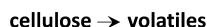
Received: February 13, 2015

Revised: April 1, 2015

Published: April 15, 2015



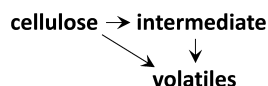
- If no, the core of the reaction model must be



- If yes, the core of the reaction model must be



- If sometimes, the core of the reaction model must be



When selecting a mathematical reaction model, it should be self-evident that the differential equations describing that model should match the words used to describe the model. If the first model is true, the reaction can be a first-order reaction, which seems to be the most common approximation. If the second or third model is true, then the relative rates must follow certain relationships. For example, for the second model to appear as a first-order reaction, either the first or second reaction must be much faster than the other so that there is only one rate-determining step. In other words, either the formation of the intermediate must be much faster than its conversion to volatiles so that essentially all the cellulose is converted to the intermediate before the second reaction becomes important, or the conversion to volatiles is so much faster than formation of the intermediate that it is barely detectable. For the third model to appear as a first-order reaction, the formation of the intermediate must either be much faster than both direct and indirect conversion to volatiles or be so slow that it is insignificant. Recognize that the dominant pathway for volatile production could change from direct to indirect or vice versa depending on the relative activation energies of the two cellulose conversion reactions.

The reaction intermediate has been variously proposed to be a melted state, a partially depolymerized chain, or some combination thereof.² Although pure melting may be possible under extremely fast heating conditions, at moderate heating it is more likely in large part due to partial depolymerization. Characterization of water-soluble intermediates continues to be an active area of research. The maximum concentration of water-solubles is 3% at 10% mass loss for 30 min at 100–350 °C¹¹ and 20% at 60% mass loss for heating at 100 °C/s to 300–750 °C.¹² The lower concentration of solubles for slow heating may be due to competitive (cross-linking) char-formation reactions that have a lower activation energy.

Some global reaction mechanisms have a very high activation energy (e.g., 58 kcal/mol¹³ and 61.7 kcal/mol¹⁴) for the formation of active cellulose, which thereby requires a very large preexponential factor in order to produce a reaction that is faster than the formation of volatiles. A similar result and controversy occurred in the study of collagen denaturation, for which the apparent activation energy is over 100 kcal/mol for a reaction that occurs at about 60 °C.¹⁵ Such kinetics were challenged,¹⁶ but the reply¹⁷ was that the separation of long chains can indeed have such high A and E_a values because of the per element contribution, including an $\exp(\Delta S/R)$ term in the preexponential factor. High activation energies have also been observed for melting of polymer gels¹⁸ and polymer glass transitions.¹⁹ So while the high activation energies for formation of activated cellulose should not be accepted without question, they cannot be dismissed out of hand, either.

MATHEMATICAL APPROACHES TO KINETIC MODELS

There are two basic approaches for optimizing the models described above. One is to write down a mass balance equation for each component coupled with rate laws for each reaction and numerically solve the reaction network. For experimental conditions that are typically modeled, the model has the form of differential equations. This is a sound approach in general, but it is hard to mathematically constrain the numerous reaction parameters to unique values. The second is to use a simpler mathematical model that captures the essence of the reaction network. The latter approach is more common in the literature and will be discussed in this section.

For a first-order reaction, the solution is trivial:

$$\text{volatiles} = F(1 - \text{cellulose}) = F(1 - e^{-k_1 t}) \quad (1)$$

where F is the fraction of cellulose converted to volatiles. Semilog plots of the reactant or $(1 - \text{products})$ must be linear at constant temperature for this model to be correct.

If the reaction intermediate is required, there are analytical solutions for isothermal conditions for both the serial reaction (case 2) and the competing pathway reaction (case 3). They have been considered in the context of oil shale pyrolysis^{20,21} and cellulose pyrolysis.¹⁴

The solutions for a strictly sequential model neglecting char and gas formation are

$$\text{cellulose} = e^{-k_1 t} \quad (2)$$

$$\text{active cellulose} = F_1 \frac{k_1}{k_2 - k_1} [e^{-k_1 t} - e^{-k_2 t}] \quad (3)$$

$$\text{volatiles} = F_1 F_2 \frac{1}{k_2 - k_1} [k_2(1 - e^{-k_1 t}) - k_1(1 - e^{-k_2 t})] \quad (4)$$

The maximum active cellulose concentration is

$$\text{max imum active cellulose} = F_1 (k_1/k_2)^{k_2/(k_2-k_1)} \quad (5)$$

and the time for maximum active cellulose concentration is

$$t_{\text{max}} = \frac{1}{(k_2 - k_1)} \ln \left(\frac{k_2}{k_1} \right) \quad (6)$$

Another property of a sequential reaction with different activation energies is that there is a temperature at which the two reaction rates are equal:

$$T_{\text{equal}} = \frac{(E_1 - E_2)}{R} \ln \left(\frac{A_1}{A_2} \right) \quad (7)$$

Far above or far below this equivalence temperature, the reaction will be close to first-order but with different rate limiting steps. Near this equivalence temperature, the reaction progression will be sigmoidal at constant temperature.

Of possible relevance to cellulose pyrolysis is that although the strictly sequential model is commonly used in oil shale pyrolysis, Ziegel and Gorman²² showed that it could not be true, because the intermediate concentration did not reach the required levels. Consequently, they considered two alternate-pathway models in which volatiles could be formed both directly from starting material and via a nonvolatile intermediate. The production of volatiles can become a

complicated function of multiple rate constants when a multistep reaction exists.

Conceptually, the alternate-pathway model can be considered as the starting material being able to react by independently breaking weak and strong bonds. At low temperatures, the weak bonds break much faster, so a substantial concentration of reaction intermediate is observed. At high temperatures, the higher activation energy of the strong bond causes them to break faster in either relative or absolute terms, so a substantially larger fraction of the conversion is directly from starting material to volatiles. The only way of testing this reaction complexity is to measure both intermediate and volatile concentrations over a wide temperature range. This is a challenge for cellulose pyrolysis, as there is no consensus yet on what active cellulose actually is.

On the other hand, if the reaction intermediate is required mechanistically, there is another class of reaction models that *might* be useful—the JMAEK (Johnson–Mehl²³–Avrami^{24–26}–Erofe'ev²⁷–Kolmogorov²⁸) model, the Prout–Tompkins model (and extensions), and the random-scission model. The JMAEK model is a geometric nucleation–growth model named after its various independent discoverers and is called by various names in different application communities. The Prout–Tompkins (PT) model is named after one of the two discovering groups and is basically an empirical model based on the logistical equation, either linear or logarithmic in time. This equation produces a sigmoidal reaction progression, which is observed in many solid-state reactions. The random-scission model is based on the pioneering work on polymer decomposition at the US National Bureau of Standards (NBS) 50–60 years ago and has recently been reformulated for use in typical thermal analysis methods. All three approaches give similar but subtly different reaction profiles. From a practical viewpoint, none are probably rigorously correct for any given application, so to the extent that all have adjustable parameters to fit data, any or all can be used beneficially for global modeling outside their rigorous conceptual origins.

Solid-state reactions ordinarily occur by the creation of a nucleation site and then the geometric growth of that nucleation site. The simplest nucleation–growth model does not recognize the overlapping consumption of reactants and leads to a continuous increase in the reaction rate with time. The JMAEK and PT models are two different approaches to modeling that growth and convergence, which leads to a sigmoidal-like conversion law.

The JMAEK model considers the merging of reaction centers, obtaining

$$\alpha = 1 - \exp(-kt^p) \quad (8)$$

where α is the fraction reacted and p is the growth dimensionality. In thermal analysis, reaction kinetics are often considered in terms of the equation

$$d\alpha/dt = k(T)f(\alpha) \quad (9)$$

In this formalism

$$f(\alpha) = p(1 - \alpha)[- \ln(1 - \alpha)]^{(p-1)/p} \quad (10)$$

The PT model is based more empirically on the logistical function. They found that the decomposition followed the equation

$$\ln\left[\frac{\alpha}{1 - \alpha}\right] = kt + c \quad (11)$$

which corresponds to the rate form

$$d\alpha/dt = k(1 - \alpha)\alpha \quad (12)$$

Šesták and Berggren²⁹ proposed an empirical equation that combines aspects of the PT and JMAEK equations:

$$d\alpha/dt = k\alpha^m(1 - \alpha)^n[- \ln(1 - \alpha)]^s \quad (13)$$

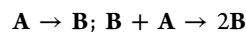
This equation has all the limits of the n th order, extended PT (ePT), and JMAEK models, although s in this equation equals $1 - 1/p$ in the JMAEK model. The inclusion of both the $(1 - \alpha)$ and $\ln(1 - \alpha)$ terms is largely redundant in terms of any modeling need. Furthermore, Brown et al.³⁰ observe that it is difficult to distinguish whether the ePT or JMAEK approaches fit any given data better, and a quantitative comparison³¹ of the two approaches given elsewhere reached a similar conclusion. However, the use of master curves as described later in this section may provide some discrimination ability.

The ePT model ($s = 0$ in eq 13) has an interesting history. Although usually cited from the 1944 paper of Prout and Tompkins on decomposition of KMnO_4 , it actually appears in the literature earlier. Austin and Rickett³² considered both the normal autocatalytic equation (eq 11) and the logarithmic analogue,

$$\ln[\alpha/(1 - \alpha)] = k \ln t + c \quad (14)$$

for analyzing decomposition kinetics of austenite—important in steel tempering. The latter worked better for them, and Prout and Tompkins³³ also found in a later paper that the logarithmic form worked better for AgMnO_4 . Avrami refers to the Austin and Rickett paper part I of his series²⁴ as a limit of his equation, and Erofe'ev³⁴ showed by series expansion and grouping that the ePT model is equivalent with the Avrami–Erofe'ev (JMAEK) model with certain ordered pairs of n and m .

An issue with some simple forms of the sigmoidal reaction models is that the initial reaction rate is zero and the reaction can never get started. This can be rectified in several ways, but it is instructive to first explore a more complete version of an autocatalytic model commonly used for energetic materials.³⁵ Consider the reaction sequence



which can be described mathematically by the relation $d\text{A}/dt = -k_1\text{A} - k_2\text{AB}$. The differential equation cast in terms of fraction reacted in the thermal analysis style is

$$d\alpha/dt = k_1(1 - \alpha)^{n_1} + k_2\alpha^m(1 - \alpha)^{n_2} \quad (15)$$

where the reaction orders are added empirically for flexibility. If we assume that $n_1 = n_2$, then

$$\begin{aligned} d\alpha/dt &= k_2(1 - \alpha)^n(\alpha^m + z) \\ &\approx k_2(1 - \alpha)^n[1 - q(1 - \alpha)]^m \end{aligned} \quad (16)$$

where $z = k_1/k_2 \approx 1 - q$. The z and q factors are basically ways of starting numerical integration with a nonzero reaction rate in the absence of an explicit initiation reaction, and they can be optimized to fit any given data set. While no analytical solution is available for these equations, a solution is available for n and m equal to 1 (the basic PT limit):

$$\alpha = 1/(e^{-kt}(1 - \alpha_0)/\alpha_0 + 1) \quad (17)$$

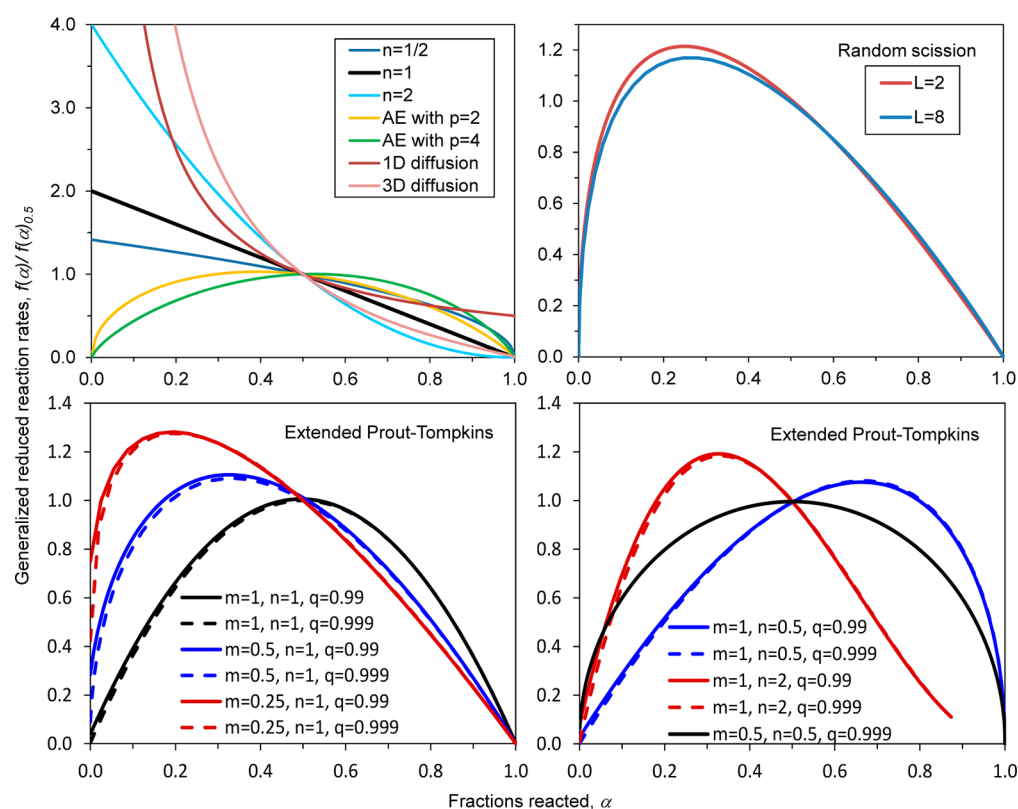


Figure 1. Normalized reaction rates for various reaction models from the thermal analysis literature.^{38,41,44} AE stands for Avrami–Erofe’ev, which is a commonly used name for the JMAEK model, and the extended Prout–Tompkins model is eq16.

where α_0 is the integration constant that provides an initial fraction reacted to get the reaction started.

That organic pyrolysis reactions occur by chain reactions has been known for a hundred years or so. By the early 1930s, detailed mechanisms³⁶ had been worked out for initiation, propagation, and termination of hydrocarbon cracking, including how to calculate the overall activation energy from the activation energies of the various steps.

The essence of any chain reaction is that there is an active center that initiates the chain, a chain propagation that generates some number of new active centers, and some sort of quenching reaction that ends the chain. Although the physical process of each step may be different for chain reaction and geometric models, the mathematics is the same unless one develops a detailed mechanistic model. For example, the number of new active centers generated in a chain reaction is analogous to the growth dimensionality in a geometric model.

The most directly relevant analogue to geopolymers pyrolysis comes from synthetic polymer pyrolysis, which was explored in great detail 50–60 years ago. Flynn and Florin³⁷ review that work, which includes lengthy NBS reports and multiple books. They summarize the main mechanisms as random main-chain scission, depolymerization, side-group reactions, and carbonization. Random chain scission is the breaking of the main chain to form smaller molecules of all sizes. The molecular weight falls, eventually forming molecules small enough to be volatile. There is no preference for monomer formation. Polyethylene and polypropylene are examples. Depolymerization is the unzipping of the polymer after an occasional break. Monomer formation is primary. Tetrafluoroethylene, α -methylstyrene, and methyl methacrylate are examples.

Flynn and Florin³⁷ review depolymerization theory and present theoretical results for various situations. Depending on the initiation location and unzipping length in the absence of chain transfer, the reaction rate vs conversion can be either deceleratory or sigmoidal. End initiation with a small zip length leads to a flat reaction rate curve. This is simply because each end is generating volatiles at a constant rate, and until most of the material is consumed, the number of ends remains constant. In contrast, random initiation with a small zip length results in an acceleratory phase, as the number of ends generating volatiles increases with time during the first phase of pyrolysis. For very large zip rates, the rate decreases with time, since a single initiation consumes the entire chain, and the number of chains decreases with time.

A relatively new addition to the common thermal analysis models is the random-scission model derived by Sanchez-Jimenez et al.³⁸ from pioneering NBS polymer degradation work by Simha and Wall.³⁹ Although Sanchez-Jimenez et al. were the first to put this in thermal analysis formalism, Burnham et al.³¹ also drew upon the work of Simha and Wall in justifying the use of the ePT model, which has a similar functional form.

Consider the case of a linear polymer for which more than one bond must be broken to form a volatile product. The rate of breaking of a single bond is given by

$$\frac{dx}{dt} = k(1 - x) \quad (18)$$

where x is the fraction of bonds broken, and the overall conversion to volatiles is given by

$$\alpha = 1 - (1 - x)^{L-1} \left[1 + x \frac{(N - L)(L - 1)}{N} \right] \quad (19)$$

where N and L are the degree of polymerization and the minimum length of polymer that is not volatile, respectively. Since normally $L \ll N$,

$$\alpha = 1 - (1 - x)^{L-1} [1 + x(L - 1)] \quad (20)$$

and

$$\frac{d\alpha}{dt} = L(L - 1)kx(1 - x)^{L-1} \quad (21)$$

So in the nomenclature of thermal analysis

$$f(\alpha) = L(L - 1)x(1 - x)^{L-1} \quad (22)$$

Sanchez-Jimenez et al.³⁸ go one step further and note that for $L = 2$, one can obtain a symbolic solution to eq 22:

$$f(\alpha) = 2(\alpha^{1/2} - \alpha) \quad (23)$$

The use of various types of reduced scale plots has been common in the solid-state reaction and thermal analysis fields for many years. Gotor et al.⁴⁰ recently introduced the concept that the activation energy of the reaction can be used to normalize the reaction rate for an arbitrary thermal history so constant temperature, constant heating rate, and any other thermal history can be plotted together to determine reaction characteristics. They proposed normalizing to the reaction rate at 50% conversion. Plots for various model reactions commonly used in the thermal analysis literature^{38,40,41} are shown in Figure 1. By interpolation, an ePT model with $m = 0.4$ has approximately the same reaction profile as a random-scission model.

One characteristic not shown in Figure 1 is that the reaction profile at a constant heating rate can become substantially narrower than a first-order reaction. This is particularly relevant to the random-scission and extended Prout–Tompkins models. Even though the normalized reaction rates for $L = 2$ and $L = 8$ are nearly superimposable for the random-scission model, the peak reaction rate is more than 5 times larger for $L = 8$,³⁸ with a corresponding narrowing of the reaction profile. Similarly, making q closer to one narrowed the reaction profile for energetic materials and was necessary to properly calculate self-heating and deflagration.³⁵ Algorithms for estimating extended Prout–Tompkins parameters by combining the activation energy estimated by Kissinger's method⁴² with the profile width relative to that of the corresponding first-order reaction are given by Braun and Burnham⁴³ and Burnham.⁴⁴

The most telling characteristic of a nucleation–growth or random-scission reaction is that it takes time to reach its maximum reaction rate at constant temperature. Although it is hard to do an isothermal experiment for pyrolysis reactions that take minutes due to apparatus heatup times and thermal lags, it is possible to come close by dropping a small sample into a well-mixed reactor having a large thermal mass. This was accomplished at Lawrence Livermore National Laboratory by dropping small samples into a fluidized bed of sand (~1:1000 mass ratio). One set of experiments involving two kerogens and polystyrene was given by Burnham et al.⁴⁵ The Anvil Points oil shale kerogen was nearly first order in this experiment and in others. The polystyrene showed a time lag of 30 s due to chemical reaction characteristics, which is long compared to the few seconds for thermal transient and gas dispersion effects

measured using n -C₁₈-doped firebrick. This sigmoidal characteristic is consistent with the polystyrene literature. The Brotherson oil shale sample shows an initial first-order devolatilization, most likely biomarkers,⁴⁶ and a larger sigmoidal devolatilization indicative of a linear polymeric structure. From this data, it is clearly indisputable that at least some, if not most, organic pyrolysis reactions are not first order.

The purpose of the foregoing review is not to advocate a particular model but rather to show that describing the reaction in certain words implies differential equations that have solutions that can be simply tested in many situations. These methods have been used extensively for materials other than cellulose. However, the broader class of possible reaction models requires numerical integration of a set of differential equations.

■ COMPLICATIONS FROM POOR TEMPERATURE MEASUREMENTS

A historical problem in all chemical kinetics is that temperature non-uniformities cause inaccurate temperature measurements. For macroscopic samples, it can be due to non-uniformity of furnaces and poorly placed thermocouples. For thermal analysis, the challenges are to measure the relationship between the sample location and the measuring device and to not have a large thermal gradient for the high heating rates common in ramped experiments. How much sample is tolerable as a function of heating rate depends on the details of the apparatus, but some guidance is available from the literature.

First, consider the location of the thermocouple. Next consider the case of the sample being large enough to have a significant thermal gradient due to an endothermic heat load. In the absence of a gas flow, measuring the temperature on the outside will overestimate the average sample temperature, and measuring the temperature on the inside will underestimate the average sample temperature. For very large samples, measuring on both the inside and outside can enable a good estimate of the average temperature, but that is not possible in typical thermal analysis. Now consider the effect of gas flow. Measuring temperature upstream will overestimate the sample temperature, and measuring downstream will have a smaller error due to the cooling of the gas flow by the sample. In all these cases, the magnitude and sign of the error depend on the details of the system. Furthermore, if the system is calibrated in such a way that the thermal lag is taken into account (e.g., Curie point calibrations with a comparable heat load at all heating rates), some thermal transients can be nulled out. This thermal compensation effect was not considered by Paulsen et al.⁴⁷ in their analysis, nor apparently was the contribution of conductive and radiative heat transfer to the sample, so their assessment of sample size effects is probably too pessimistic.

Second, consider how much temperature error is tolerable. There are three basic types of laboratory temperature errors that can affect kinetic parameters and influence the reliability of extrapolation to times and temperatures outside the measurement regime: (1) a constant shift in all measurement temperatures, (2) a temperature error that varies systematically with temperature or heating rate, and (3) random errors. Burnham et al.⁴⁸ demonstrated the effect of errors 1 and 2. A consistent error of 6 °C (e.g., item 1) had a negligible error on the activation energy and led to a consistent 5–6 °C prediction error even over large temperature extrapolations. In contrast, an error that increased from zero to 6 °C over a decade of heating rate (~40 °C overall shift) caused about a 7 kcal/mol error in

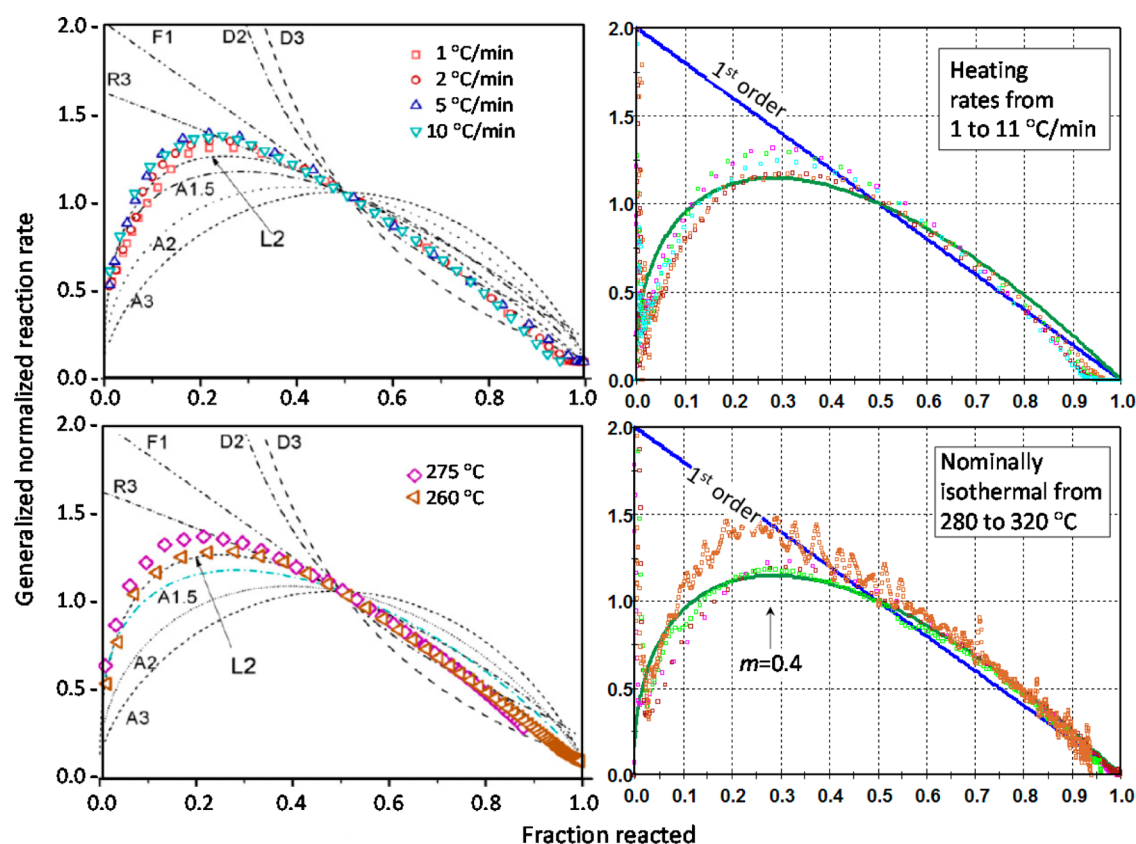


Figure 2. Examples of generalized reduced reaction rate plots for cellulose. Left: Adapted from Sanchez-Jimenez et al.,⁶⁰ Copyright 2013, with permission from Elsevier. Not shown are comparable plots for thermal histories designed to maintain a constant reaction rate. Right: Calculated from the data of Capart et al.⁵⁹

activation energy and a compensating error of >100 in the pre-exponential factor, resulting in >20 °C error for large temperature extrapolations. The implication here is that thermal lags at the highest heating rate should be less than 2 °C to obtain the activation energy within 2 kcal/mol, which should be sufficient for most applications. The random error issue is discussed elsewhere.^{49,50} Replicates at the extreme temperatures or heating rates are more important than many intermediate temperatures because they have the largest leverage on the kinetic parameters.

The issue of temperature calibration received substantial attention in the recent International Confederation for Thermal Analysis and Calorimetry (ICTAC) Kinetics Committee recommendations on collecting kinetics data.⁵¹ Two of the references contained therein addressed sample sizes for polymers⁵² and energetic materials,⁵³ respectively. Lyon et al.⁵² calculated the thermal profiles across polymers as a function of sample size. The maximum recommended sample size ranged from 300 mg at 1 °C/min to 1 mg at 40 °C/min for heats of decomposition ~ 1 kJ/g. Burnham and Weese⁵³ found for HMX, which has an exotherm of 4.2 MJ/g, that the maximum sample size was 0.5 mg at 1 °C/min, which is consistent with an extrapolation of the results of Lyon et al.⁵²

Cellulose measurements in the literature have not always followed practices that lead to temperature measurements of the quality needed for kinetic measurements. The decomposition enthalpy of cellulose is comparable to that of the polymers considered by Lyon et al.,⁵² so their guidance is directly relevant. Antal et al.⁵⁴ found that at 65 °C/min the reaction profile was significantly broader when using 9 mg than

when using 0.3 mg. They attributed the broadening to thermal lag and non-uniformity in the sample. This result agrees with the recommendations of Lyon et al.⁵² Similarly, Grønli et al.⁵⁵ found that at 40 °C/min, reduction of the sample from 0.94 mg to 0.11 mg decreased the peak decomposition temperature by 8 °C/min, which seems larger than expected but could be the case for a particular instrument. Lin et al.³ found that the peak temperature at 150 °C/min depended strongly on sample size over the range of 2.5–24 mg. Although the rate of change of the peak pyrolysis temperature lessened going from 2.5 to 7.8 mg, it is likely that the 2.5 mg sample still had a thermal lag. Their thermal model estimated a maximum thermal lag of about 25 °C for an 8 mg sample, which would indicate that a sample at least 10 times smaller would be necessary. An extrapolation of the curve of Lyon et al.⁵² would suggest a maximum sample of ~ 0.1 mg at that heating rate. Lin et al.³ also found a maximum thermal lag of ~ 5 °C for an 8 mg sample at 15 °C/min, which would be on the border of acceptability of the plot of Lyon et al.⁵² The calculated thermal lag at 1 °C/min was negligible for that size sample, which would agree with all recommendations.

Combining these various studies together, a rule of thumb for cellulose would be that a product of the heating rate and sample size below 10 mg °C/min would ensure having a thermal lag of less than 1 °C. The round robin described by Grønli et al.⁵⁵ used slightly larger samples, which suggests that there may be a few degrees error in those results. The 10 mg °C/min criterion is consistent with the result in that paper that 0.1 mg is better than 0.9 mg at 40 °C/min. Experiments using larger samples should be viewed with caution, although

depending on the relative locations of the thermocouple and sample, the way the sample is dispersed (layer vs pile), the carrier gas (N_2 vs He), and the way the instrument is calibrated, the acceptable sample could be a few times greater.

■ THE NATURE OF THE CELLULOSE PYROLYSIS CURVE

The early days of pyrolysis (>40 years ago) usually involved analyzing the data by an n th-order reaction, and the data might be either isothermal or a single constant heating ramp. The NBS work on polymer degradation described earlier was an exception. In the last 20 years, nucleation–growth models developed for solid state reactions have been used increasingly to model organic pyrolysis reactions.

A major controversy in cellulose pyrolysis over the past 20 years is whether rapid cellulose pyrolysis is a first-order reaction or some type of sigmoidal reaction. The primary protagonist for the first-order reaction was and still is Antal, who argues that the evidence for a reaction intermediate was an artifact due to thermal lag.^{54,56,57} There is certainly no doubt that thermal lag can cause an acceleratory period in nominally isothermal experiments, but the question is really whether there is a chemical acceleratory period after that thermal transient is removed by experimental or computational methods.

Much of the argument about whether cellulose pyrolysis follows a sigmoidal or first-order rate law has been over interpretation of experiments at a constant heating rate. It is critical to understand that the sequential reaction profile, the random-scission reaction profile, and the JMAEK and Prout–Tompkins nucleation–growth reaction profiles are not readily distinguished from a first-order reaction by the profile shape alone. A more characteristic feature of the sigmoidal reactions is that the reaction profile is significantly narrower than a first-order reaction. Consequently, if the reaction is sigmoidal, fitting the reaction rate from a single heating rate will give an activation energy and frequency factor higher than the true values in order to fit the narrowness of the reaction profile. This characteristic has been known for more than 25 years.^{45,58}

The reason this history is important for cellulose pyrolysis interpretation is that the papers of Antal and collaborators all use fitting to a single heating rate to determine the activation energy. From the preceding paragraph, it is obvious that if the true reaction is sigmoidal due to a sequential or nucleation–growth or random-scission mechanism, the activation energies of 53–58 kcal/mol in the Antal papers will be too high. In contrast, three recent papers^{7,59,60} using isothermal and ramped heating in a thermogravimetric analyzer (TGA) used a nucleation–growth or random-scission model and an iso-conversional model to obtain activation energies in the range of 46–48 kcal/mol. Part of Figure 5 of Sanchez-Jimenez et al.⁶⁰ is reproduced in Figure 2 along with comparable plots recalculated from the data of Capart et al.⁷ using $m = 0.4$. One might argue that the highest heating rates and temperatures have some thermal lag, but the near coincidence of the various thermal histories, including very slow heating, argues strongly that thermal lag has a negligible influence on the shape of the curves. The shape of the generalized reduced rate curves is unambiguously consistent with either a random-scission model or a nucleation–growth model (JMAEK shown as AE for Sanchez-Jimenez and ePT for Capart; also compare to ePT curves in Figure 1). The discrepancies at very low and high conversion are due to drying and char devolatilization, respectively.

Other recent papers support the need for a sigmoidal reaction model of some sort. Kim and Eom⁶¹ used TGA and reduced-time plots to choose a reaction model and determine an Avrami exponent of 3.7, which is highly acceleratory. Barud et al.⁶² used a nonlinear isoconversional approach to confirm that cellulose pyrolysis followed the Avrami–Erofe'ev model with an exponent p of 1.63 and an E_a of about 44 kcal/mol. That Avrami exponent corresponds to an ePT value for m of 0.45. Matsuoka et al.⁶³ provide both chemical reaction and thermal decomposition results supportive of a nucleation–growth model, in this case related to the more labile character of the reducing ends at the boundaries of the crystalline domains. All this work was preceded by two substantially earlier papers proposing a nucleation–growth model,^{64,65} although the activation energies in those papers appear to be a little too low.

A particularly interesting recent paper concerning the role of thermal lag and chemical kinetics is that of Lin et al.³ Using sample sizes that put them far into the thermal lag regime at their higher heating rates, they use a combined heat transport and chemical reaction model to derive an E_a of 47.3 kcal/mol by simultaneously matching all heating rates. Even more interesting is that inspection of their measured and calculated reaction curves indicates that the measured profile is a little sharper than the calculated curves. Digitizing their curves, Kissinger's method⁴² gives an E_a of only 36.7 kcal/mol. However, after making an average temperature correction at each heating rate according to their thermal model and then fitting to a nucleation–growth model, the resulting ePT parameters are $A = 1.27 \times 10^{15} \text{ s}^{-1}$, $E_a = 47.5 \text{ kcal/mol}$, $n = 1.36$, and $m = 0.22$ for $q = 0.99$, which are consistent with a mildly sigmoidal reaction.

Returning to the work of the Antal group, it is important to understand that the practice of fitting kinetic models to a single heating rate was specifically addressed and strongly discouraged as unreliable to nonsensical in papers addressed to the thermal analysis community. In the 1960–2000 time frame, there was a common practice of fitting many reaction models to a single heating rate and then choosing the best model according to the lowest residuals. However, the A and E_a values from the various models varied all over the map and had no particular relationship to reality. Such practice was abandoned in the 1980s in the petroleum geochemistry field,^{43,66} but it continued in the thermal analysis field. This practice was thoroughly discredited by Vyazovkin and Wight in the late 1990s^{67,68} and then by the ICTAC Kinetics Committee in two seminal papers.^{41,69} Although a few stragglers still derive chemical kinetics from a single heating rate, the thermal analysis community has largely abandoned that practice.

The A and E_a values reported for the cellulose round robin are shown in Figure 3. Two problems are apparent. One is that A and E_a are different for the two heating rates. This is a concern because they should be an invariant property of the reaction. Second, the pre-exponential factors are extremely high, and one would expect values of order 10^{14} s^{-1} as pointed out by Agarwal et al.⁷⁵ The reason for the slightly lower A and E_a at 40 °C/min is attributed to a broader profile related to minor thermal lag effects, and that gives rise to a compensation relationship. However, a greater concern is that when E_a was constrained to the same value at different heating rates, A varied typically by a factor of 3 at 1 and 65 °C/min.⁵⁴ This violates the basic premise of the Arrhenius equation.

The reason for the compensation relationship evident in the individual determinations for that study is often debated in the

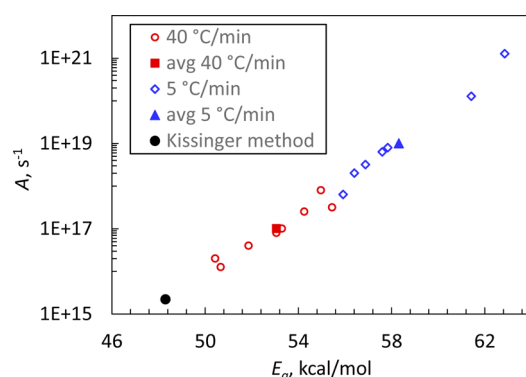


Figure 3. Arrhenius parameters determined in a round robin study of cellulose pyrolysis.⁵⁵

literature. Although there are theoretical reasons why the compensation relationship has a mechanistic meaning, e.g., for catalyst efficiency, the compensation effect is more often merely a reflection of experimental error—usually temperature measurement errors—or the use of an improper kinetic model. For a given reaction rate at a single temperature, there are an infinite number of $A-E_a$ pairs that satisfy that rate and any given model. Only by changing temperature substantially can one isolate the true $A-E_a$ pair, and the statistical spread is a natural consequence of imperfect temperature measurements. That all the reported $A-E_a$ pairs fall on a line indicate that the data are generally of the same family, and the difference at the two heating rates is probably a reflection of the slightly broader reaction profiles at the higher heating rate due to thermal transients.

One can get a better estimate of the true A and E_a by using Kissinger's method on the average temperature at maximum reaction rate (T_{\max}) values at the two heating rates. This analysis gives a plausible A of $2.2 \times 10^{15} \text{ s}^{-1}$ and an E_a of 48.3 kcal/mol that is consistent with the theoretical estimates and experimental values discussed above. Furthermore, if one calculates reaction curves from the reported first-order reaction parameters at each heating rate and then fits the two reaction profiles simultaneously to a nucleation–growth model, one obtains $A = 2.6 \times 10^{15} \text{ s}^{-1}$, $E_a = 48.3 \text{ kcal/mol}$, $n = 0.97$, and $m = 0.16$ for $q = 0.99$. These parameters are very similar to those derived from the data of Lin et al.³ A comparison of the measured and calculated fractions reacted are shown in Figure 4, and the agreement is excellent.

One recent paper supplies a twist to this otherwise consistent picture. Samuelsson et al.⁸ found that sample sizes of 4.0 and 9.9 mg gave sigmoidal kinetics with an E_a of $\sim 43 \text{ kcal/mol}$. However, a sample size of 1.6 mg produced first-order kinetics with an E_a of $\sim 52 \text{ kcal/mol}$. Data kindly supplied to us was reanalyzed by Friedman's method and model fitting, and results very similar to theirs were obtained. Also significant is that their T_{\max} values were the same at 2 °C/min and diverged by 5–8 °C at 15 °C/min. The divergence indicates that thermal gradients were present for the larger samples at the higher heating rates, but correspondingly, the convergence indicates that thermal gradients were not present at the slower heating rates. Applying a relaxed limit of $\sim 20 \text{ mg } ^\circ\text{C/min}$, gradients should be insignificant for all sample sizes at their lowest heating rate and for their smallest sample size at all heating rates, which is consistent with their T_{\max} evidence.

While a superficial look at this result might conclude that thermal gradients are responsible for the change from first-

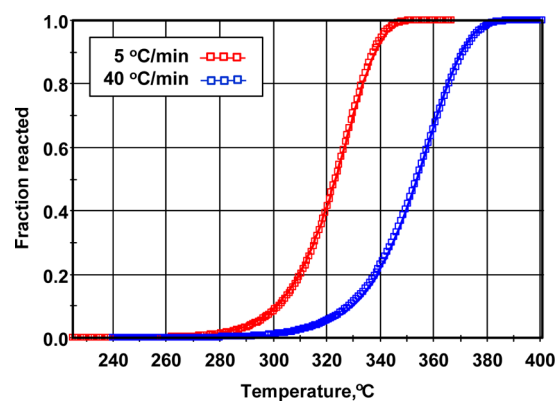


Figure 4. Comparison of a nucleation–growth model fitted simultaneously to both heating rates (5 and 40 °C/min) reported by Grønli et al.⁵⁵

order to sigmoidal kinetics, a closer examination indicates that it must be due to other causes, such as mass transfer resistance, which would lead to delayed evaporation and more char from the larger samples.⁷⁰ This is because for the larger samples, all heating rates provided the same sigmoidal character, and if thermal gradients were responsible, the faster heating rates would have sigmoidal character and the slowest one not. In fact, master plots show that the slower heating rate experiments actually have greater sigmoidal character. This would be consistent with lower product vapor pressures due to lower temperatures. This explanation is also consistent with larger char yields for larger samples and slower heating rates. It also points out that the kinetics of product generation and product evolution are not identical, and this issue deserves more study.

■ INSIGHTS FROM RECENT MECHANISTIC CALCULATIONS

It has been known for many years that the primary monomeric pyrolysis product of cellulose pyrolysis is levoglucosan. The longstanding questions are the mechanism by which that occurs, e.g., directly from cellulose or via an active cellulose intermediate,² and whether other products are secondary products from levoglucosan or direct products from either cellulose or active cellulose.^{47,71–73} The most significant development concerning cellulose pyrolysis in the past decade is the conclusion that cellulose pyrolysis probably occurs by a concerted mechanism,^{74–77} and depending on how the reaction is carried out, the mechanistic steps can be catalyzed by water or OH groups on neighboring molecules.^{78,79}

Agarwal et al.⁷⁵ found a depolymerization reaction with an E_a of 20 kcal/mol that they propose could be the driving force for irreversible conversion of crystalline cellulose to liquid material at temperatures above 260 °C. They then suggest a corrected E_a of about 41 kcal/mol for formation of a precursor to levoglucosan. They also make the point that activation energies for the overall reaction must be in the 45–48 kcal/mol range to have physically plausible A values of 10^{13} to 10^{14} s^{-1} . This conclusion is consistent with E_a derived in the previous section using a sigmoidal reaction model.

Seshadri et al.⁷⁹ explored a variety of mechanisms associated with cellulose decomposition using transition-state theory supported by quantum chemistry and statistical mechanics calculations. They first found a water-assisted isomerization of α - to β -glucose via a linear aldose having an E_a of 23 kcal/mol. This transformation was thought to relate to the conversion of

crystalline cellulose to an amorphous intermediate. This intermediate would then decompose to levoglucosan by a hydroxyl-catalyzed concerted mechanism having an E_a of about 46 kcal/mol. This activation energy is consistent with both the conclusion of Agarwal et al.⁷⁵ and the sigmoidal reaction model parameters.

Broadbelt and co-workers reported a detailed mechanistic model for fast pyrolysis of neat glucose-based carbohydrates including glucose, cellobiose, maltohexaose, and cellulose by integrating findings obtained through experiments and theoretical calculations.^{74,76} 342 reactions of 103 species were presented in the mechanistic model to describe the decomposition of cellulosic polymer chains, reactions of intermediates, and formation of 67 low molecular weight compounds at the mechanistic level and each elementary reaction step was specified in terms of Arrhenius parameters.

Of particular relevance here is that this mechanism includes a hydrolysis reaction having an E_a of 34.0 kcal/mol leading to a liquid intermediate, a primary initiation reaction (concerted random cleavage) having an E_a of about 53.5 kcal/mol, depropagation (unzipping) reactions with activation energies of 51.5 kcal/mol, and other unimolecular and bimolecular reactions. Their figures show that the molar composition of chains and various rate components are not consistent with an overall first-order reaction, in that species and rates do not decay exponentially with time. Instead, they show the characteristic rise and fall associated with a sequential reaction mechanism.⁷⁷

This conclusion is supported by analysis of the disappearance of condensed phase components other than char using conventional kinetic analysis using Kinetics2015 software (<http://geoisochem.com/software/kinetics2015/index.html>). Fractions reacted corresponding to weight loss were calculated at temperatures of 400, 500, and 600 °C. First, results from isoconversional kinetic analysis using Friedman's method⁸⁰ are shown in Table 1. Note that the E_a and A decline with

Table 1. Kinetic Parameters from Isoconversional Analysis of Synthetic Weight Loss Data from the Broadbelt Group Mechanism

fraction reacted, α	$\ln[A(1 - \alpha)^n]$	A, s^{-1}	E_a , kcal/mol	std dev, kcal/mol
0.1	32.855	2.06×10^{14}	51.76	0.05
0.2	33.190	3.24×10^{14}	51.85	0.03
0.3	33.433	4.73×10^{14}	52.01	0.13
0.4	33.512	5.97×10^{14}	52.01	0.11
0.5	33.189	5.19×10^{14}	51.53	0.16
0.6	31.702	1.47×10^{14}	49.53	1.14
0.7	28.745	1.02×10^{13}	45.74	1.88
0.8	29.235	2.49×10^{13}	47.54	0.06
0.9	28.178	1.73×10^{13}	47.16	0.68

conversion as the mix of chemical reactions changes. The characteristic values of fast pyrolysis of neat cellulose are about $1 \times 10^{14} s^{-1}$ and 50 kcal/mol, significantly lower than advocated by Antal and collaborators as shown in Figure 3. Also note that the nonzero standard deviation is because even at fixed conversion, the reaction shows non-first-order character.

Next, the data were fitted to an ePT reaction (eq 16) by nonlinear regression. The results of such fitting depend on what objective function is minimized, and a range of possibilities is shown in Table 2. In this case, "cum" indicates a fit to the cumulative reacted, "rate" indicates a fit to the reaction rate, and "cum + rate" indicates a fit simultaneously to the reaction rate and cumulative reacted. RSS is the residual sum of squares. The overall summary is that reaction has substantial sigmoidal character with A of about $1 \times 10^{15} s^{-1}$ and E_a of 52 kcal/mol. In comparing the results of Tables 1 and 2, it is important to understand that the nucleation–growth A is larger than a first-order A by a factor of about $1/(1 - m + 0.17m^2)$, and given that a shift of E_a by one kcal/mol is compensated by a factor of 2 change in A , the parameters are more consistent than first might appear.

A comparison of the simulated and fitted reaction data is shown in Figure 5 for the last entry in Table 2. It is quite possible to obtain good fits over the very wide temperature range with kinetic parameters that are consistent with those in the underlying mechanism.

More important, Figure 6 shows that the data show clear evidence for an initial acceleratory phase characteristic of a sigmoidal reaction. The maximum reaction rate occurs close to mid conversion. For comparison, a first-order reaction has its maximum normalized rate of 2.0 at 0.0 fraction reacted and follows a straight trajectory to zero at complete reaction (Figure 1). The simulated data show a break in the slope that does not occur in the real data (Figure 2), suggesting that a broader spectrum of reactions occur in reality.

A concern is that when applied to constant heating rates, the Broadbelt group mechanism predicts higher conversion temperatures (slower reaction rates) than observed in Figure 4. Mid conversion is predicted at 397 °C for 5 °C/min and 432 °C for 40 °C/min, which are about 80 °C higher than measured. This corresponds to a slower reaction rate from the mechanistic model of a factor of about 100. The difference is smaller but still substantial when compared to the data of Reynolds and Burnham,⁶⁵ so perhaps sample differences can account for some of the difference.

Another possible cause of a difference is the lower volatility of the primary pyrolysis products under typical TGA conditions. However, mass transfer resistances based strictly on vapor pressure would cause a discrepancy in the opposite direction. Furthermore, to the extent that there are residual thermal gradients in the TGA experiments, they would also

Table 2. Kinetic Parameters for the ePT Nucleation–Growth Model Derived from Synthetic Weight Loss Data

fit to	q	A, s^{-1}	E_a , kcal/mol	m	n	rate RSS	cum RSS
cum	0.999	8.19×10^{14}	51.10	0.693	1.60	1.773	0.149
rate	0.999	1.46×10^{15}	52.11	0.683	1.42	1.191	0.341
rate + cum	0.999	1.29×10^{15}	51.87	0.694	1.49	1.224	0.249
cum	0.99	9.95×10^{14}	51.11	0.841	1.69	1.536	0.146
rate	0.99	1.98×10^{15}	52.17	0.856	1.61	1.018	0.310
rate + cum	0.99	1.69×10^{15}	51.91	0.863	1.64	1.046	0.236

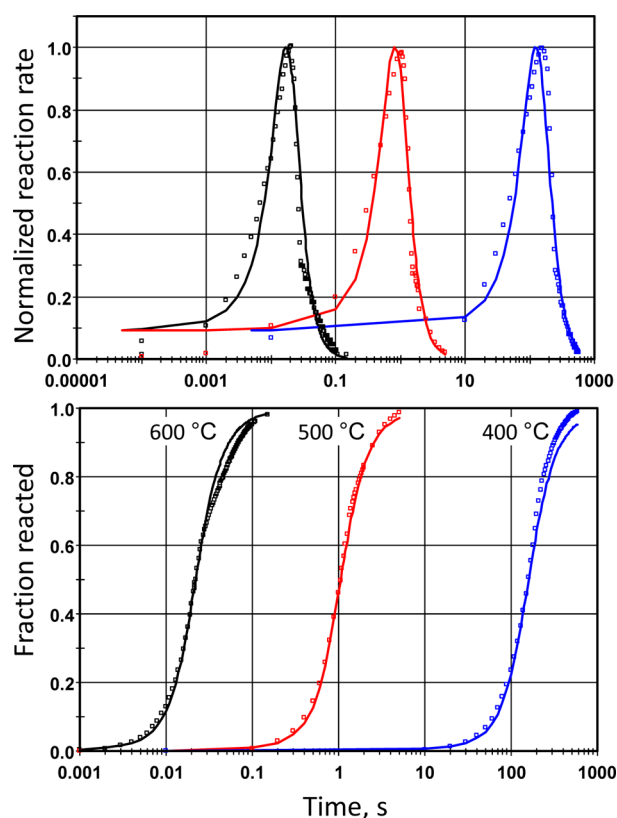


Figure 5. Comparison of simulated and fitted reaction rates and fractions reacted for the Broadbelt group mechanistic reaction model of cellulose pyrolysis.

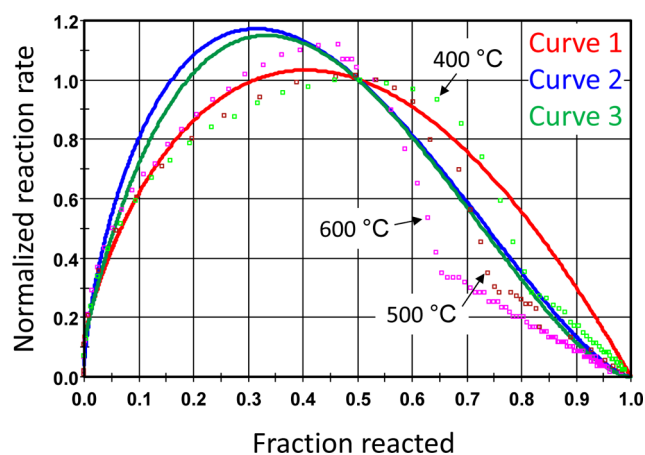


Figure 6. Reaction rate versus fraction reacted normalized at mid conversion. The mechanistic calculations at three temperatures are indicated by square points. All global kinetic curves (colored lines, which are independent of temperature) used $A = 1 \times 10^{15} \text{ s}^{-1}$ and $E_a = 53 \text{ kcal/mol}$. Curve 1: $m = 0.7$, $n = 1$, $q = 0.99$. Curve 2: $m = 0.85$, $n = 1.65$, $q = 0.99$. Curve 3: $m = 0.69$, $n = 1.5$, $q = 0.999$.

cause a discrepancy in the opposite direction. And even if the discrepancy were in the right direction, it is the wrong magnitude. The data of both Lin et al.³ and Grønli et al.⁵⁵ find that a factor of 10 increase in sample up from when heat transfer effects are negligible causes a change (increase, by the way) of 8 °C or less in the peak reaction temperature at typical TGA heating rates.

On the other hand, if the nucleation–growth kinetics derived from Grønli et al.⁵⁵ are used to predict the pyrolysis time at 500

°C, the reaction is complete in about 0.1 s, which is about 10 times faster than calculated by the Broadbelt-group mechanistic model.⁷⁷ In fact, if the TGA kinetics are correct, the pyrolysis is not actually isothermal at 500 °C when using a commonly used pyrolyzer. Depending on sample size, the time constant for sample heatup in the experiments of Zhang et al.⁸¹ ranged from 0.1 to 0.3 s, and the time constant for heating the sample cup is about 1 s. Using the TGA nucleation–growth kinetics with thermal histories following a $1 - e^{-t/\tau}$ law with time constants of 0.1, 0.32, and 1 s predicts 50% reaction times and temperatures of 1.7, 0.76, and 0.29 s and 440, 455, 472 °C, respectively. Consequently, it is not certain that the reaction is as isothermal as proposed by Zhang et al.⁸¹

The discrepancy between the mechanistic calculations and experiment would go away if OH catalysis increased the concerted initiation reaction rate. Mechanistic calculations of Seshadri et al.^{78,79} indicate that increases of 100 and 10 at 300 and 500 °C, respectively, are plausible indeed. Consequently, it is plausible that incorporation of such catalytic effects in the more comprehensive Broadbelt-group mechanism might lead to a mechanistic model that is able to rectify perceived differences between TGA and more rapid pyrolysis.

In fact, kinetic models for other systems have been successful at diverse time and temperature scales for transformation of kerogen in oil shale retorting and natural petroleum formation,^{82,83} cracking of hydrocarbons for industrial olefin production and survival in petroleum reservoirs,^{84,85} and for aging and deflagration of energetic materials.^{35,86} Experience for other materials has shown that for complex kinetic systems, in the absence of a discontinuity such as a phase change, the mechanism usually changes in a rather smooth way over temperature such that the temperature-dependence can be modeled successfully by an effective activation energy that has absorbed the continuously changing weights of the underlying fundamental reactions.

CONCLUSIONS

Cellulose pyrolysis kinetics has a diverse history, but recent mechanistic modeling has confirmed a broad range of experimental work indicating that the reaction involves a reaction intermediate prior to volatile generation. Once problems with thermal transients and lags are removed and proper kinetic analysis methods are used, the most probable experimental apparent E_a for rapid cellulose pyrolysis appears to be in the vicinity of 47 kcal/mol. This is consistent but slightly lower than the E_a of ~50 kcal/mol for levoglucosan generation by a concerted reaction. However, the concerted reaction can be catalyzed by water or neighboring OH groups depending on how the reaction is carried out, which would lower the apparent E_a to ~47 kcal/mol. Simulated data from a detailed mechanistic model (Broadbelt group) are consistent with a sigmoidal reaction and give global kinetic parameters that are similar to those derived from thermal analysis data using sigmoidal reaction models, even though remaining discrepancies suggest the need for OH-catalyzed initiation in the mechanistic models.

At the same time, this convergence shows that the first-order reaction constants derived from a single heating rate are not correct. As has been shown numerous times in the thermal analysis literature, fitting a first-order reaction to a sequential or nucleation–growth or random-scission reaction profile will yield A and E_a values higher than the true values. This is because this type of reaction often has the same profile shape as a first-order reaction but is significantly narrower. In the case of

cellulose, this erroneous procedure yields A values that are too large to be physically reasonable—much larger than the $\sim 10^{14} \text{ s}^{-1}$ values in the mechanistic models that have been developed recently using rate parameters derived from transition state theory.

AUTHOR INFORMATION

Corresponding Author

*E-mail: akburnham@yahoo.com.

Present Address

§(A.K.B.) Consultant, 4221 Findlay Way, Livermore, CA 94550.

Notes

The authors declare no competing financial interest.

ACKNOWLEDGMENTS

This work was supported by Genie Energy and Total S. A. and by the Department of Energy (DOE) Office of Energy Efficiency and Renewable Energy (EERE) through the Office of Biomass Program, Grant DEEE0003044. Financial support from the Institute for Sustainability and Energy at Northwestern (ISEN) is also gratefully acknowledged. The authors thank P. Westmoreland for a presentation at the 248th ACS meeting that inspired this paper. The authors also thank L. Samuelsson and R. Moriana for sharing their data so we could understand their results more fully.

REFERENCES

- (1) White, J. E.; Catallo, W. J.; Legendre, B. L. Biomass pyrolysis kinetics: A comparative critical review with relevant agricultural residue case studies. *J. Anal. Appl. Pyrolysis* **2011**, *91*, 1–33.
- (2) Lédé, J. Cellulose pyrolysis kinetics: An historical review on the existence and role of intermediate active cellulose. *J. Anal. Appl. Pyrolysis* **2012**, *94*, 17–32.
- (3) Lin, Y.-C.; Cho, J.; Tomsett, G. T.; Westmoreland, P. R.; Huber, G. W. Kinetics and mechanism of cellulose pyrolysis. *J. Phys. Chem. C* **2009**, *113*, 20097–20107.
- (4) Shafizadeh, F. Introduction to pyrolysis of biomass. *J. Anal. Appl. Pyrolysis* **1982**, *3*, 283–305.
- (5) Diebold, J. P. A unified, global model for the pyrolysis of cellulose. *Biomass Bioenergy* **1994**, *7*, 75–85.
- (6) Gaur, S.; Reed, T. B. Prediction of cellulose decomposition rates from thermogravimetric data. *Biomass Bioenergy* **1994**, *7*, 61–67.
- (7) Capart, R.; Zhesami, L.; Burnham, A. K. Assessment of various kinetic models for the pyrolysis of a microgranular cellulose. *Thermochim. Acta* **2004**, *417*, 79–89.
- (8) Samuelsson, L. N.; Moriana, R.; Babler, M. U.; Ek, M.; Engvall, K. Model-free rate expression for thermal decomposition processes: The case of microcrystalline pyrolysis. *Fuel* **2015**, *143*, 438–447.
- (9) Laksmanan, C. M.; Gal-Or, B.; Hoelscher, H. E. Production of levoglucosan by pyrolysis of carbohydrates. *Ind. Eng. Chem. Prod. Res. Devel.* **1969**, *8*, 261–267.
- (10) Lakshmanan, C. M.; Hoelscher, H. E. Production of levoglucosan by pyrolysis of carbohydrates. *Ind. Eng. Chem. Prod. Res. Devel.* **1970**, *9*, 57–59.
- (11) Yu, Y.; Liu, D.; Wu, H. Characterization of water-soluble intermediates from slow pyrolysis of cellulose at low temperatures. *Energy Fuels* **2012**, *26*, 7331–7339.
- (12) Gong, X.; Yu, Y.; Gao, X.; Xu, M.; Wu, H. Formation of anhydro-sugars in the primary volatiles and solid residues from cellulose fast pyrolysis in a wire-mesh reactor. *Energy Fuels* **2014**, *28*, 5204–5211.
- (13) Bradbury, A. G. W.; Sakai, Y.; Shafizadeh, F. A kinetic model for pyrolysis of cellulose. *J. Appl. Polym. Sci.* **1979**, *23*, 3271–3280.
- (14) Lin, Y.; Cho, J.; Davis, J. M.; Huber, G. W. Reaction-transport model for the pyrolysis of shrinking cellulose particles. *Chem. Eng. Sci.* **2012**, *74*, 160–171.
- (15) Miles, C. A.; Burjanadze, T. V. The kinetics of thermal denaturation of collagen in unrestrained rate tail tendon determined by DCS. *J. Mol. Biol.* **1995**, *345*, 437–446.
- (16) Engel, J.; Bachinger, H. P. Cooperative equilibrium transitions coupled with a slow annealing step explain the sharpness and hysteresis of collagen folding. *Matrix Biol.* **2000**, *19*, 235–244.
- (17) Miles, C. A.; Bailey, A. J. Response to Engel and Bachinger's critique of collagen denaturation as a rate process. *Matrix Biol.* **2001**, *20*, 263–265.
- (18) Chen, K.; Baker, A. N.; Vyazovkin, S. Formation and thermal behavior of polystyrene and polystyrene/clay gels. *Macromol. Chem. Phys.* **2008**, *209*, 2367–2373.
- (19) Vyazovkin, S.; Sbirrazzuoli, N.; Dranca, I. Variation in activation energy of the glass transition for polymers of different dynamic fragility. *Macromol. Chem. Phys.* **2006**, *207*, 1126–1130.
- (20) Braun, R. L.; Rothman, A. J. Oil-shale pyrolysis: kinetics and mechanism of oil production. *Fuel* **1975**, *54*, 129–131.
- (21) Miknis, F. P.; Turner, T. F. The bitumen intermediate in isothermal and nonisothermal decomposition of oil shales. In *Composition, Geochemistry and Conversion of Oil Shales*; Snape, C., Ed.; NATO ASI Series, Vol. 455, Kluwer: Dordrecht, 1995; pp 295–311.
- (22) Ziegel, E. R.; Gorman, J. W. Kinetic modeling with multiresponse data. *Technometrics* **1980**, *22*, 139–151.
- (23) Johnson, W.; Mehl, R. Reaction kinetics in processes of nucleation and growth. *Trans. AIME* **1939**, *135*, 416–442.
- (24) Avrami, M. Kinetics of phase change. I. General theory. *J. Chem. Phys.* **1939**, *7*, 1103–1112.
- (25) Avrami, M. Kinetics of phase change. II. Transformation-time relation for random distribution of nuclei. *J. Chem. Phys.* **1940**, *8*, 212–224.
- (26) Avrami, M. Kinetics of phase change. III. Granulation, phase change, and microstructure. *J. Chem. Phys.* **1940**, *8*, 177–184.
- (27) Erofe'ev, B. V. *C. R. Dokl. Akad. Sci. USSR* **1946**, *52*, 511–514.
- (28) Kolmogorov, A. A statistical theory for the recrystallization of metals. *Akad. Nauk. SSSR, Izv. Ser. Matem.* **1937**, *1*, 355–359.
- (29) Šesták, J.; Berggren, G. Study of the kinetics of the mechanism of solid-state reactions at increasing temperatures. *Thermochim. Acta* **1971**, *3*, 1–12.
- (30) Brown, M. E. The Prout-Tompkins rate equation in solid-state kinetics. *Thermochim. Acta* **1997**, *300*, 93–106.
- (31) Burnham, A. K.; Braun, R. L.; Coburn, T. T.; Sandvik, E. I.; Curry, D. J.; Schmidt, B. J.; Noble, R. A. An appropriate kinetic model for well-preserved algal kerogens. *Energy Fuels* **1996**, *10*, 49–59.
- (32) Austin, J. B.; Rickett, R. L. Kinetics of the decomposition of Austenite at constant temperature, AIME Technical publication 964, 1938, 20 pp. *Trans. AIME* **1939**, *135*, 396–415.
- (33) Prout, E. G.; Tompkins, F. C. The thermal decomposition of silver permanganate. *Trans. Far. Soc.* **1946**, *42*, 468–472.
- (34) Erofe'ev, B. V. In *Reactivity of Solids, Proceedings of the 4th International Symposium*; Amsterdam, 1960; Elsevier: Amsterdam, 1961; pp 273–282.
- (35) Burnham, A. K.; Weese, R. K.; Wemhoff, A. P.; Maienshein, J. L. A historical and current perspective on predicting thermal cookoff behavior. *J. Therm. Anal. Calorim.* **2007**, *89*, 407–415.
- (36) Rice, F. O.; Herzfeld, K. F. The thermal decomposition of organic compounds from the standpoint of free radicals. VI. The mechanism of some chain reactions. *J. Am. Chem. Soc.* **1934**, *56*, 284–289.
- (37) Flynn, J. H.; Florin, R. E. Degradation and pyrolysis mechanisms. In *Pyrolysis and GC in Polymer Analysis*; Liebman, S. A., Levy, E. J., Eds.; Marcel Dekker: New York, 1985; pp 149–208.
- (38) Sanchez-Jimenez, P. E.; Perez-Maqueda, L. A.; Perejon, A.; Criado, J. M. A new model for the kinetic analysis of thermal degradation of polymers driven by random scission. *Polym. Degrad. Stab.* **2010**, *95*, 733–739.

- (39) Simha, R.; Wall, L. A. Kinetics of chain depolymerization. *J. Phys. Chem.* **1952**, *56*, 707–715.
- (40) Gotor, F. J.; Craido, J. M.; Malek, J.; Koga, N. Kinetic analysis of solid-state reactions: The universality of master plots for analyzing isothermal and nonisothermal experiments. *J. Phys. Chem. A* **2000**, *104*, 10777–10782.
- (41) Vyazovkin, S.; Burnham, A. K.; Criado, J. M.; Perez-Maqueda, L. A.; Popescu, C.; Sbirrazzuoli, N. ICTAC recommendations for performing kinetic computations on thermal analysis data. *Thermochim. Acta* **2011**, *520*, 1–19.
- (42) Kissinger, H. E. Reaction kinetics in differential thermal analysis. *Anal. Chem.* **1957**, *29*, 1702–1706.
- (43) Braun, R. L.; Burnham, A. K. Analysis of chemical reaction kinetics using a distribution of activation energies and simpler models. *Energy Fuels* **1987**, *1*, 153–161.
- (44) Burnham, A. K. Application of the Šesták–Berggren equation to organic and inorganic materials of practical interest. *J. Therm. Anal. Calorim.* **2000**, *69*, 895–908.
- (45) Burnham, A. K.; Braun, R. L.; Taylor, R. W.; Coburn, T. T. Comparison of isothermal and nonisothermal pyrolysis data with various rate mechanisms: Implications for kerogen structure. *Prep. ACS Div. Petrol. Chem.* **1989**, *34* (1), 36–41.
- (46) Burnham, A. K.; Clarkson, J. E.; Singleton, M. F.; Wong, C. M.; Crawford, R. W. Biological markers from Green River kerogen decomposition. *Geochim. Cosmochim. Acta* **1982**, *46*, 12443–1251.
- (47) Paulsen, A. D.; Mettler, M. S.; Dauenhauer, P. J. The role of sample dimension and temperature on cellulose pyrolysis. *Energy Fuels* **2013**, *27*, 2126–2134.
- (48) Burnham, A. K.; Braun, R. L.; Gregg, H. R.; Samoun, A. M. Comparison of methods for measuring kerogen pyrolysis rates and fitting kinetic parameters. *Energy Fuels* **1987**, *1*, 452–458.
- (49) Peters, K. E.; Burnham, A. K.; Walters, C. C. Petroleum generation kinetics: one- vs. multiple-heating ramp open-system pyrolysis. *AAPG Bull.* **2015**, *99*, 591–616.
- (50) Burnham, A. K. Obtaining reliable phenomenological chemical kinetic models for real-world applications. *Thermochim. Acta* **2014**, *597*, 35–40.
- (51) Vyazovkin, S.; Chrissafis, K.; Di Lorenzo, M. L.; Koga, N.; Pijolet, M.; Roduit, B.; Sbirrazzuoli, N.; Sunol, J. J. ICTAC Kinetics Committee recommendations for collecting thermal analysis data for kinetic computations. *Thermochim. Acta* **2014**, *590*, 1–23.
- (52) Lyon, R. E.; Safronova, N.; Senese, J.; Stoliarov, S. I. Thermokinetic model of sample response in nonisothermal analysis. *Thermochim. Acta* **2012**, *545*, 82–89.
- (53) Burnham, A. K.; Weese, R. K. *Thermal Decomposition Kinetics of HMX*; LLNL Report UCRL-TR-204262-Rev-1; Lawrence Livermore National Laboratory: Livermore, CA, 2004; <https://e-reports-ext.llnl.gov/pdf/314135.pdf>.
- (54) Antal, M. J.; Varhegyi, G.; Jakab, E. Cellulose pyrolysis kinetics: revisited. *Ind. Eng. Chem. Res.* **1998**, *37*, 1267–1275.
- (55) Grønli, M.; Antal, M. J.; Varhegyi, G. A round-robin study of cellulose pyrolysis kinetics by thermogravimetry. *Ind. Eng. Chem. Res.* **1999**, *38*, 2238–2244.
- (56) Antal, M. J.; Varhegyi, G. Cellulose pyrolysis kinetics: The current state of knowledge. *Ind. Eng. Chem. Res.* **1995**, *34*, 703–717.
- (57) Narayan, R.; Antal, M. J. Thermal lag, fusion, and the compensation effect during biomass pyrolysis. *Ind. Eng. Chem. Res.* **1996**, *35*, 1711–1721.
- (58) Dollimore, D.; Evans, T. A.; Lee, Y. F.; Wilburn, F. W. Correlation between the shape of a TG/DTG curve and the form of the kinetic mechanism which is applying. *Thermochim. Acta* **1992**, *198*, 249–257.
- (59) Sanchez-Jimenez, P. E.; Perez-Maqueda, L. A.; Perejon, A.; Pascual-Cosp, J.; Benitez-Guerrero, M.; Criado, J. M. An improved model for the kinetic description of the thermal degradation of cellulose. *Cellulose* **2011**, *18*, 1487–1498.
- (60) Sanchez-Jimenez, P. E.; Perez-Maqueda, L. A.; Perejon, A.; Criado, J. M. Generalized masterplots as a straightforward approach for determining the kinetic model: The case of cellulose pyrolysis. *Thermochim. Acta* **2013**, *552*, 54–59.
- (61) Kim, S.; Eom, Y. Estimation of kinetic triplet of cellulose pyrolysis reaction from isothermal kinetic results. *Kor. J. Chem. Eng.* **2006**, *23*, 409–414.
- (62) Barud, H.; Riberio, C.; Capella, J.; Crespi, M. S.; Ribeiro, S.; Messadeq, Y. Kinetic parameters for thermal decomposition of microcrystalline, vegetal, and bacterial cellulose. *J. Therm. Anal. Calorim.* **2011**, *105*, 421–426.
- (63) Matsuoka, S.; Kawamoto, H.; Saka, S. What is active cellulose in pyrolysis? An approach based on reactivity of cellulose reducing end. *J. Anal. Appl. Pyrolysis* **2014**, *106*, 138–146.
- (64) Dollimore, D.; Holt, B. Thermal degradation of cellulose in nitrogen. *J. Polym. Sci.* **1973**, *11*, 1703–1711.
- (65) Reynolds, J. G.; Burnham, A. K. Pyrolysis decomposition kinetics of cellulose-based materials by constant heating rate micropyrolysis. *Energy Fuels* **1997**, *11*, 88–97.
- (66) Ungerer, P.; Pelet, R. Extrapolation of the kinetics of oil and gas formation from laboratory experiments to sedimentary basins. *Nature* **1987**, *327*, 52–54.
- (67) Vyazovkin, S.; Wight, C. A. Isothermal and nonisothermal kinetics in solids: In search of ways toward consensus. *J. Phys. Chem. A* **1997**, *101*, 8279–8284.
- (68) Vyazovkin, S.; Wight, C. A. Kinetics in solids. *Annu. Rev. Phys. Chem.* **1997**, *48*, 125–149.
- (69) Brown, M. E.; Maciejewski, M.; Vyazovkin, S.; Nomen, R.; Sempere, J.; Burnham, A.; et al. Computational Aspects of Kinetic Analysis. Part A: The ICTAC Kinetics Project—data, methods and results. *Thermochim. Acta* **2000**, *355*, 125–143.
- (70) Bai, X.; Brown, R. C. Modeling the physiochemistry of levoglucosan during cellulose pyrolysis. *J. Anal. Appl. Pyrolysis* **2014**, *105*, 363–368.
- (71) Di Blasi, C. Numerical simulation of cellulose pyrolysis. *Biomass Bioenergy* **1994**, *7*, 87–98.
- (72) Zhang, X.; Yang, W.; Blasiak, W. Thermal decomposition mechanism of levoglucosan during cellulose pyrolysis. *J. Anal. Appl. Pyrolysis* **2012**, *96*, 110–119.
- (73) Patwardhan, P. R.; Dalluge, D. L.; Shanks, B. H.; Brown, R. C. Distinguishing primary and secondary reactions of cellulose pyrolysis. *Bioresour. Technol.* **2011**, *102*, 5265–5269.
- (74) Mayes, H. B.; Broadbelt, L. H. Unraveling the reactions that unravel cellulose. *J. Phys. Chem. A* **2012**, *116*, 7098–7106.
- (75) Agarwal, V.; Dauenhauer, P. J.; Huber, G. W.; Auerbach, S. M. Ab initio dynamics of cellulose pyrolysis: Nascent decomposition pathways at 327 and 600 °C. *J. Am. Chem. Soc.* **2012**, *134*, 14958–14972.
- (76) Zhou, X.; Nolte, M. W.; Mayes, H. B.; Shanks, B. H.; Broadbelt, L. J. Experimental and mechanistic modeling of fast pyrolysis of neat glucose-based carbohydrates. 1. Experiments and development of a detailed mechanistic model. *Ind. Eng. Chem. Res.* **2014**, *53*, 13274–13289.
- (77) Zhou, X.; Nolte, M. W.; Shanks, B. H.; Broadbelt, L. J. Experimental and mechanistic modeling of fast pyrolysis of neat glucose-based carbohydrates. 2. Validation and evaluation of the mechanistic model. *Ind. Eng. Chem. Res.* **2014**, *53*, 13290–13301.
- (78) Seshadri, V.; Westmoreland, P. R. Concerted reactions and mechanism of glucose pyrolysis and implications for cellulose kinetics. *J. Phys. Chem. A* **2012**, *116*, 11997–12013.
- (79) Seshadri, V.; Fahey, P. J.; Westmoreland, P. R. Role of pericyclic reactions in the pyrolysis of cellulose and hemicellulose, Paper ENFL-133, 248th National Meeting of the American Chemical Society, San Francisco, CA, August 2014.
- (80) Friedman, H. L. Kinetics of thermal degradation of char-forming plastics from thermogravimetry. Application to a phenolic plastic. *J. Polym. Sci., Part C* **1964**, No. 6, 183–195.
- (81) Zhang, J.; Nolte, M. W.; Shanks, B. H. Investigation of primary reactions and secondary effects from the pyrolysis of different celluloses. *ACS Sustainable Chem. Eng.* **2014**, *2*, 2820–2830.

(82) Burnham, A. K.; Braun, R. L. Development of a detailed model of petroleum formation, destruction, and expulsion from lacustrine and marine source rocks. *Org. Geochem.* **1990**, *16*, 27–39.

(83) Walters, C. C.; Freund, H.; Keleman, S. R.; Peczak, P.; Curry, D. J. Predicting oil and gas compositional yields via chemical structure-chemical yield modeling (CS-CYM): Part 2—Application under laboratory and geologic conditions. *Org. Geochem.* **2007**, *38*, 306–322.

(84) Jackson, K. J.; Burnham, A. K.; Braun, R. L.; Knauss, K. G. Temperature and pressure dependence of *n*-hexadecane cracking. *Org. Geochem.* **1995**, *23*, 941–953.

(85) Burnham, A. K.; Sanborn, R. H.; Gregg, H. R. Thermal dealkylation of dodecylbenzene and dodecylcyclohexane. *Org. Geochem.* **1998**, *28*, 755–758.

(86) Burnham, A. K.; Weese, R. K.; Andrzejewski, W. J. Kinetics of HMX and CP decomposition and their extrapolation for lifetime assessment. In *36th Intl. Annual Conference and 32nd International Pyrotechnics Seminar*, Karlsruhe, Germany, June 28 – July 1, 2005. Also, Lawrence Livermore National Laboratory Report UCRL-CONF-210589, 2005.